AD-A115 204 TECHNOLOGY ASSOCIATES INC WEST LAFAYETTE IN F/G 20/6
FABRICATION AND EXPERIMENTAL TECHNIQUES IN INTEGRATED OPTICS.(U)
SEP 81 C CHEN N00163-81-M-1798
UNCLASSIFIED NAC-TR-2318 NL

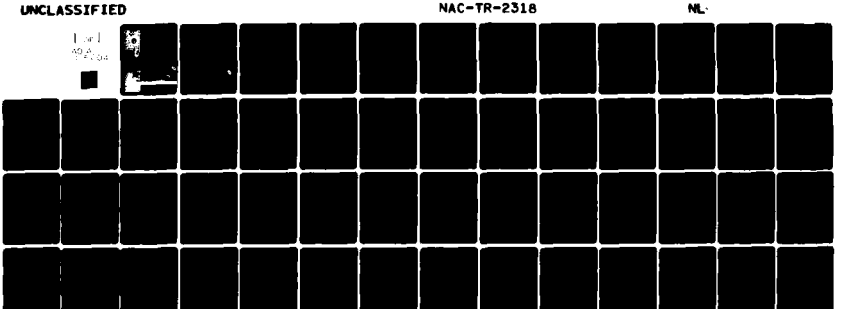

END
DATE FILMED
7-82
DTIC

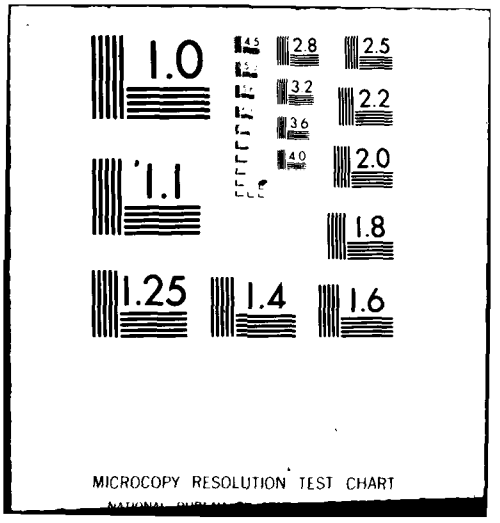
1.0
1.1
1.25
1.4
1.6
1.8
2.0
2.2
2.5
2.8
3.2
3.6
4.0
MICROCOPY RESOLUTION TEST CHART

(12)

TR-2318
SEPTEMBER 1981

NAC publication
APPLIED RESEARCH DEPARTMENT

FABRICATION AND EXPERIMENTAL TECHNIQUES IN INTEGRATED OPTICS

FINAL TECHNICAL REPORT TR-2318
CONTRACT NUMBER NOO163-81-M-1798

Approved for Public Release; Distribution Unlimited

Prepared by:

Chin Lin Chen

Technology Associates, Inc.
West Lafayette, Indiana 47906

NAVAL AVIONICS CENTER
INDIANAPOLIS, INDIANA 46218

FABRICATION AND EXPERIMENTAL TECHNIQUES IN INTEGRATED OPTICS

Prepared by

Chin-Lin Chen

September 15, 1981

Final Report

for

Contract N00163 81 M 1798

U.S. Naval Avionics Center
Indianapolis, Indiana

Technology Associates. Inc.
208 Pawnee Drive
West Lafayette, IN 47906

UNCLASSIFIED

SECURITY CLASSIFICATION OF THIS PAGE (When Data Entered)

REPORT DOCUMENTATION PAGE		READ INSTRUCTIONS BEFORE COMPLETING FORM
1. REPORT NUMBER NAC TR-2318	2. GOVT ACCESSION NO. AD-A115 204	3. RECIPIENT'S CATALOG NUMBER
4. TITLE (and Subtitle) Fabrication and Experimental Techniques in Integrated Optics		5. TYPE OF REPORT & PERIOD COVERED Final Report Feb 1981 - Sep 1981
		6. PERFORMING ORG. REPORT NUMBER
7. AUTHOR(s) Chin-Lin Chen		8. CONTRACT OR GRANT NUMBER(s) N00163-81-M-1798
9. PERFORMING ORGANIZATION NAME AND ADDRESS Technology Associates, Inc. West Lafayette, Indiana 47906		10. PROGRAM ELEMENT, PROJECT, TASK AREA & WORK UNIT NUMBERS
11. CONTROLLING OFFICE NAME AND ADDRESS Naval Avionics Center 6000 E. 21st Street Indianapolis, Indiana 46218		12. REPORT DATE September 1981
		13. NUMBER OF PAGES 44
14. MONITORING AGENCY NAME & ADDRESS(if different from Controlling Office)		15. SECURITY CLASS. (of this report) Unclassified
		15a. DECLASSIFICATION/DOWNGRADING SCHEDULE

16. DISTRIBUTION STATEMENT (of this Report)

Approved for Public Release; Distribution Unlimited

17. DISTRIBUTION STATEMENT (of the abstract entered in Block 20, if different from Report)

18. SUPPLEMENTARY NOTES

19. KEY WORDS (Continue on reverse side if necessary and identify by block number)

20. ABSTRACT (Continue on reverse side if necessary and identify by block number)

A program to investigate the characteristics of integrated optical components, coupling between optical waveguides and other optical components and waveguide fabrication technology was initiated in February 20, 1981 for the Naval Avionics Center under Contract N00163-81-M-1798. The work performed under this contract is summarized in this report. The Navy technical monitor was Dr. K. J. Jones.

DD FORM 1 JAN 73 1473 EDITION OF 1 NOV 65 IS OBSOLETE
S/N 0102-014-6601 |

UNCLASSIFIED

SECURITY CLASSIFICATION OF THIS PAGE (When Data Entered)

Abstract (Con'd)

A prism coupling measurement system was modified and improved. Numerical techniques for computing the refractive index and the thickness of the optical films from the experimental data are discussed. Techniques based on optical fibers and TV cameras for measuring the waveguide attenuation, and techniques related to end-fire coupling and near infrared radiation are considered. Methods for fabricating solution-deposited waveguides and waveguides on glass, lithium niobate and lithium tantalate substrates are also reviewed.

FABRICATION AND EXPERIMENTAL TECHNIQUES IN INTEGRATED OPTICS

Chin-Lin Chen

Technology Associates, Inc.

W. Lafayette, IN 47906

ABSTRACT

A program to investigate the characteristics of integrated optical components, coupling between optical waveguides and other optical components and waveguide fabrication technology was initiated in February 20, 1981 for Naval Avionics Center under contract N00163 81 M 1798. The work performed under this contract is summarized in this report. The Navy technical monitor was Dr. K. J. Jones.

A prism coupling measurement system was modified and improved. Numerical techniques for computing the refractive index and the thickness of the optical films from the experimental data are discussed. Techniques based on optical fibers and TV cameras for measuring the waveguide attenuation, and techniques related to end-fire coupling and near infrared radiation are considered. Methods for fabricating solution-deposited waveguides and waveguides on glass, lithium niobate and lithium tantalate substrates are also reviewed.

TABLE OF CONTENTS

1.0 INTRODUCTION

Since the useful bandwidth of a coherent source is proportional to its oscillating frequency, and the frequency of a laser radiating in the visible or near infrared spectra is of the order of 10^{14} Hz, its useful bandwidth is tremendous. Many optical devices and systems have been conceived to take advantage of the tremendous bandwidth of lasers. However, the weight, size and alignment problems of bulk optical devices and their susceptibility to mechanical vibrations, air turbulence and temperature fluctuation prevent these devices from becoming practical. Recently interest has turned to integrated optical devices and systems, since many of the problems associated with bulk optical devices are absent in the integrated or guided-wave devices.

In February 1981, an integrated optical device program was initiated at Technology Associates, Inc. for Naval Avionics Center (NAC). The objectives were to provide the technical support for the enhancement of NAC's in-house integrated optics (IO) activities in upgrading its experimental facilities and evaluation capabilities, and to assist NAC personnel in screening, evaluating and assessing appropriate IO material, components and technologies for specific systems of current and future interst to NAC.

Optical waveguides are the basic building blocks of any IO system. Optical components can be built from, and optical subsystems can be connected by the optical waveguides. The potential exists that all optical components and associated electronics may be fabricated on a common substrate.

Waves can be coupled into or out of the waveguides via prism, end-fire or grating coupling. So far as experimental investigations are concerned, prism couplers are probably the most versatile tool for coupling radiation into or out of waveguides and for characterizing guided modes. On the other hand, end-fire coupling is the most reliable. The prism (Figure 1) and end-fire (Figure 2) coupling schemes will be discussed in Sections 2 and 3 respectively. Grating coupling, not attempted in this work, will not be discussed in this report. The effective index of refraction and the attenuation constant are two basic and important characteristics of optical waveguides. Techniques to estimate these waveguide parameters are discussed in Sections 4 and 5. Experiments involving infrared or near infrared radiation are discussed in Section 6. Methods of fabricating practical optical waveguides are presented in Section 7.

2.0 PRISM COUPLING

A dielectric slab waveguide consisting of a substrate region with an index of refraction n_s, a film region of an index n_f, and a cover region with an index n_c, is the simplest possible optical waveguide structure. Many modes can be supported by the structure, depending upon the free-space wavelength λ, the thickness h of the firm, and the values of n_s, n_f and n_c. Let $N_{eff,m}$ be the effective index of refraction of the m-th guided mode, then $N_{eff,m}$ is related to these parameters via the dispersion relation [1, 2]:

$$\frac{2\pi h}{\lambda}\sqrt{n_f^2 - N_{eff,m}^2} = \Psi_m(n_f, n_s, n_c, N_{eff,m}) \tag{1}$$

where

$$\Psi_m(n_f, n_s, n_c, N_{eff,m}) = m\pi + \phi_s(n_f, n_s, N_{eff,m}) + \phi_c(n_f, n_c, N_{eff,m}) \tag{2}$$

$$\phi_s(n_f, n_s, N_{eff,m}) = \arctan\left[\left(\frac{n_f}{n_s}\right)^{2\rho}\left(\frac{N_{eff,m}^2 - n_s^2}{n_f^2 - N_{eff,m}^2}\right)^{1/2}\right] \tag{3}$$

$$\phi_c(n_f, n_c, N_{eff,m}) = \arctan\left[\left(\frac{n_f}{n_c}\right)^{2\rho}\left(\frac{N_{eff,m}^2 - n_c^2}{n_f^2 - N_{eff,m}^2}\right)^{1/2}\right] \tag{4}$$

and $\rho = 0$ for TE modes and $\rho = 1$ for TM modes.

2.1 Basic principle of prism coupling:

If a prism with an index n_p and an angle ε is placed next to the film, (see inserts of Figures 3 and 4) and an optical beam is incident upon the boundary between the film and the prism at an angle such that the projection of the phase velocity of the incoming beam in the prism matches exactly with c/N_{eff}, c being the speed of light in vacuum, of the m-th guided mode, then the m-th guided mode will be excited. This is the basic principle of prism coupling. The angle of incidence α or α', n_p, ε and N_{eff} are related by the relations below [1, 2]:

$$N_{eff} = \sin\varepsilon(n_p^2 - \sin^2\alpha)^{1/2} + \cos\varepsilon \sin\alpha \tag{5}$$

$$N_{eff} = \sin\varepsilon(n_p^2 - \sin^2\alpha')^{1/2} - \cos\varepsilon \sin\alpha' \tag{6}$$

The angles α, α' and ε are defined in the inserts to Figures 3 and 4.

2.2 Design considerations for prism couplers:

The key component of a prism coupler is, of course, the prism. The following points should be taken into account in selecting prisms:

(1) The prism should be as small as practical.

(2) The prism material should be as hard as possible to minimize the effects of scratching and chipping [2].

(3) The index of the prism should be somewhat larger, not merely slightly larger, than the index of the film, e.g., $n_p > n_f + 0.1$ or $n_p > n_f + 0.2$.

(4) To avoid spurious response due to repeated reflections from the prism surfaces, one should avoid prisms with angles of 30°, 45°, 60°, 90° or other rational fractions of 360° [2].

(5) If a half-prism, as depicted in Figures 1, 3 and 4, is used, the angle at the corner where the guided modes are launched should be sharp and well defined.

(6) The prism should have a flat top, rather than a sharp apex, so that pressure can be applied uniformly to the prism.

A possible design of prism is shown in Figure 5. For a flint glass prism (with $n_p = 1.75$) of the shape shown in Figure 5, the dependence of N_{eff} as functions of α or α' calculated from (5) or (6), are shown in Figure 3. If the prism is made of an uniaxial crystal like rutile (TiO_2) with its optic axis parallel to the edge of 91.0°, i.e., perpendicular to the figure shown, the extraordinary index $n_e = 2.87$ should be used for n_p.

Figure 4 depicts the relationship between N_{eff} and α or α' for such a rutile prism. Theoretically, coupling to substrates with N_{eff} values ranging from 1.4179 to 2.7036 can be achieved with the rutile prism and these values correspond to the coupling angles of $\alpha' = 90.°$ and $\alpha = 90.°$ respectively. In reality, the useful range is limited to 1.7295 ($\alpha' = 40.°$) to 2.6112 ($\alpha = 50.°$) region.

2.3 Operations of prism couplers:

In addition to a finite number of guided modes, a waveguide structure can support a continuum of radiation modes in the cover (air) region above the film and the substrate region below the film. These fields are referred to as the air and substrate modes respectively. The air mode has an oscillatory field distributions in all regions and has an effective index of refraction N_{eff} smaller than n_c. When N_{eff} is increased beyond n_c, there is the substrate mode which has an exponentially decaying field distribution in the cover region and oscillatory field distributions in the film and substrate regions. For the guided modes, $n_s < N_{eff} < n_f$, and the field decays exponentially in the air as well as the substrate region.

As a specific example, consider a waveguide consisting of a Corning 7059 glass film ($n_f = 1.555$) of thickness $h = 1.0$ μm and a substrate of pyrex glass ($n_s = 1.45$), of thickness of 0.1 cm. So far as the guided modes are concerned, the pyrex glass can be considered as infinitely thick. Two TE modes may be supported by the Corning 7059/pyrex structure with $N_{eff} = 1.5356$, and 1.4780. Suppose a glass prism with an index of $n_p = 1.75$ as shown in Figure 5 is used in the experiment. For $\alpha' > 27.°$, the air mode is excited.

Although the air mode is reflected from the substrate-air boundary, the reflection coefficient is small ($|\rho|^2 = 0.034$). If the laser beam is not blocked by any objects, it would emerge behind the pyrex glass. As the incident angle is increased with $\alpha' < 27.°$, or $\alpha < 10.4°$, the substrate mode is excited. The optical beam is totally reflected at the air-substrate boundaries. As a result, the beam is trapped in the pyrex glass. A dot appears at each point where the reflection occurs. Since the reflection is very efficient, with $|\rho|^2 = 1.$, a series of dots become visible. The distance between dots is a function of the thickness of substrate and will vary with α. For a pyrex glass of thickness of 0.1 cm, the distance between dots on the same boundary would vary from 0.10 cm to 1.27 cm as the angle changes from $\alpha' = 25.°$ to $\alpha = 10.0°$. As α approaches 13.6°, a continuous streak would appear, and this is the TE_1 mode with $N_{eff} = 1.4780$. When α is increased to 20.°, TE_0 mode with $N_{eff} = 1.5356$ would be excited.

From the above discussion, three points helpful to the proper interpretation of, and the successful operation of the prism coupling experiments become obvious:

(1) If possible, there should be no reflective object behind the substrate. Thus the air mode, if it is excited, will not be reflected. If this cannot be done, then, the space behind the substrate should be made accessible. By probing the space behind the substrate, one can differentiate the air mode reflected by the object behind the substrate from the substrate mode reflected by the boundary of the substrate.

(2) From the coupling angle where a series of dots begins to appear, one can use (5) or (6) to estimate the index of refraction of the substrate.

(3) As the coupling angle is changed, the distance between dots increases. The limiting case should be very close to the highest guided mode.

3.0 END-FIRE COUPLING

As mentioned previously, end-fire coupling, also known as butt coupling, is one of three methods available for coupling light into or out of an optical waveguides. As implied by the name, light is coupled into the waveguide through the end surface of the waveguide, as shown in Figure 2. In any optical waveguide, energy is concentrated in a thin layer, with a thickness of the order of a few wavelengths at most near the waveguide surface. The region near the corner of the waveguide is critical to end-fire coupling. Techniques have been developed specifically to polish the corner region of the substrate [3]. In connection with this work, a jig for polishing the end surfaces of optical waveguides has been designed and is to be used in conjunction with the existing polishing facility at NAC. This work is currently in progress.

3.1 Transformation of Gaussian beams by lens or lenses:

To achieve maximum coupling into the optical waveguide, the cross section and beam divergence of the incoming optical beam must match that of the waveguide. The optical beam emitted by a HeNe laser is typically of the Gaussian form. In particular the irradiance distribution of a

TEM_{00} Gaussian beam is given by $I_0 e^{-2r^2/\omega^2}$. The beam radius ω is defined as the radius where the irradiance is reduced to e^{-2} of its peak value I_0 at the beam center ($r = 0$). The beam radius ω_o (or diameter) at the beam waist, i.e., the point with the smallest beam radius (or diameter), is usually specified. In the Fraunhofer zone, the full angle of divergence is $2\lambda/(\pi\omega_o)$. For example, a Spectra Physics Model 145 laser has a beam diameter, of 0.5 mm and the beam diverges at full angle of 1.7 mrad. For these lasers, the beam waist is usually located at the output mirror.

A simple lens with a focal length of f can be used to change the beam radius. Let ω_{oa} and ω_{ob} be the radii of the beam waists of the incoming and outgoing beams as shown in Figure 6. ω_{oa}, ω_{ob} and their locations z_a and z_b with respect to the lens are related by

$$\frac{1}{\omega_{ob}^2} = \frac{1}{\omega_{oa}^2}\left(1 - \frac{z_a}{f}\right)^2 + \left(\frac{\pi\omega_{oa}}{f\lambda}\right)^2 \tag{7}$$

$$z_b = f + \frac{(z_a - f)f^2}{(z_a - f)^2 + (\pi\omega_{oa}^2/\lambda)^2} \tag{8}$$

where λ is the wavelength of the radiation [4]. If the beam waist ω_{oa} of the incoming beam is located at the front focal point of the lens, i.e., $z_a = f$, then the beam waist ω_{ob} is located at the back focal point $z_b = f$ and has a value

$$\omega_{ob} = \frac{f\lambda}{\pi\omega_{oa}} \tag{9}$$

For example, a lens with a focal length of 10 cm will transform a HeNe

laser beam (λ = 0.633 μm) with ω_{oa} of .25 mm to a beam with ω_{ob} = 80.59 μm.

Since the cross section of a planar waveguide is thin and wide, it may be necessary to use a cylindrical lens to transform the circular optical beam into an elliptical shape. The above equations may be used twice, one for the major axis and one for the minor axis.

The beam collected by a microscope objective or a lens may be too wide for some application. Two lenses, with focal lengths f_1 and f_2 and spaced at a distance $f_1 + f_2$, may be used to change the beam diameter by a factor of f_2/f_1, as shown in Figure 1. By choosing $f_2 < f_1$, the beam diameter is reduced. If $f_2 > f_1$, on the other hand, the beam is expanded. If a small pinhole is inserted at the common focal point of these two lenses, the lens-pinhole combination also acts as a spatial filter.

3.2 Horns for channel waveguides:

Typically, a channel waveguide is 3 to 6 μm wide and 1 to 2 μm thick. Thus channel waveguides are thin and narrow. Although the prism coupling or the end-fire coupling may be used to couple light into a channel waveguide, it is difficult to align the optical beam with respect to the channel waveguide. To relieve the alignment difficulty, a horn structure may be used to transform a planar waveguide to a channel waveguide gradually. Linearly, exponentially or parabolically tapered horns have been proposed by various authors [5 - 9]. As explained by Burns, Milton and Lee [8], the most practical horn is of the parabolic shape. For parabolic horns, the width W of the horn is given by

$$W = \sqrt{2k\lambda_g z + W_o^2} \tag{10}$$

where k is a constant and $\lambda_g = \lambda/N_{eff}$ is the local effective guide wavelength of the channel waveguide. W_o and other parameters are as shown in Figure 7. Unless the channel width, W, is very narrow such that the lowest order mode (in the x-direction as shown in Figure 7) is near to its cutoff point, λ_g can be approximated by λ_o/n_f [8]. As a specific example, again consider a HeNe laser with a beam diameter of 0.5 mm (ω_o = 250 μm) at its beam waist. Two lenses with $f_1 = 16\ f_2$ and spaced at a distance of $f_1 + f_2$ (Figure 1) can be used to reduce the beam radius to 15.6 μm. The beam diameter at the entrance point is 31.2 μm. Therefore W_{max} = 40 μm is chosen. Horns have been designed to transform W_{max} = 40 μm to channel waveguides of width 5, 10 and 20 μm respectively. Suppose that the channel waveguides and the tapering horns are to be built on photoresist waveguides with n_f = 1.6. With the selection of k = 0.8, all parameters of (10) are specified. The equations describing the horns for 5, 10 and 20 μm channel waveguides are respectively:

$$W^2 = 25.0 + 0.6328\ |z|, \qquad 0 \leq z \leq 2488.9\ \mu m \tag{11}$$

$$W^2 = 100.0 + 0.6328\ |z| \qquad 0 \leq z \leq 2369.6\ \mu m \tag{12}$$

$$W^2 = 400. + 0.6328\ |z|, \qquad 0 \leq z \leq 1895.7\ \mu m \tag{13}$$

For z = 0, W = 5 μm, 10 μm and 20 μm respectively, and W = 40 μm when z exceeds the values specified in (11), (12) or (13).

4.0 FILM INDEX AND THICKNESS

One of the most useful features of prism coupling is the relationship between α (or α') and N_{eff}. When α or α' is measured experimentally, and when n_p and ϵ are known, N_{eff} can be computed from (5) and (6). This feature, in conjunction with the dispersion relationship (1), can be used to estimate n_f and h.

For a waveguide, n_s, n_c and λ are usually known while n_f and h are unknown. If one of the coupling angles is measured and N_{eff} is computed from (5) or (6), we have one equation ((1)) yet two unknowns. There is insufficient information to solve for n_f and h. When two or more coupling angles are determined, the index n_f and thickness h of the thin film can be evaluated, provided that the indices of the substrate and the cover, n_s and n_c, are known. Cases where three or more waveguide modes are determined have to be treated differently from the cases where two waveguide modes are determined. In either case, considerable numerical computation is needed to deduce the final results from the experimentally measured data. A computer program written to carry out the necessary iteration and computation is listed in the Appendix. The theoretical foundation and the algorithm of the computer program are explained in this section. Also included are typical results obtained by the computer program. The input and output instructions are contained in the program MAIN. Additional functions of the program MAIN and various subroutines will be explained in the following sections.

4.1 Waveguides with two modes measured:

Suppose that two coupling angles are determined and $N_{eff,m}$ with $m = \mu$ and ν are computed. Then, substituting $N_{eff,\mu}$ and $N_{eff,\nu}$ into (1) and

rearranging the resultant equations, we obtain

$$n_f^2 = \frac{(N_{eff,\mu})^2 \psi_\nu^2 - (N_{eff,\nu})^2 \psi_\mu^2}{\psi_\mu^2 - \psi_\nu^2} \tag{14}$$

This is a nonlinear equation for n_f and a simple iteration scheme can be used to solve for n_f. Specifically, a trial value for n_f is assumed and (14) is used to compute a new n_f. If the new n_f differs from the old n_f considerably, the new n_f is used to compute a newer n_f. This process is repeated until a satisfactory accuracy is achieved. Once n_f is known, it is a simple matter to solve for h from (1). The computation for N_{eff} from α is carried out at the beginning of the program MAIN. The second part of program MAIN is related to the iteration for n_f and the simple calculation for h.

4.2 Waveguides with three or more modes measured:

The cases where three or more waveguide modes are measured, assuming the waveguide has three or more modes, are much more complicated. Suppose that M coupling angles are measured, with $M \geq 3$. Each measured coupling angle corresponds to a value for $N_{eff,m}$, which in turn leads to an equation with a specific value for $N_{eff,m}$. There are M equations ($M \geq 3$) and yet there are only two unknowns. One cannot solve for the unknowns from these equations unless M-2 equations are redundant. In the ideal situation where the experimental results are infinitely precise and without error, M-2 equations will be redundant. In any real experiment, however, there will be

experimental error or inaccuracy; n_f and h cannot be determined from the measured coupling angles. Instead of "solving" for n_f and h from $N_{eff,m}$, the best estimates for n_f and h are sought. Reasonable values of n_f, h are assumed and used in conjunction with the known values of n_s and n_c to compute the effective index of refraction from the dispersion relation (1). The effective index of refraction so obtained is labeled as $N_{eff,m}(n_f,h)$. The values of n_f and h are then searched so that $N_{eff,m}$ match with $N_{eff,m}(n_f,h)$. Following Ulrich and Torge [2], an error sum is defined as:

$$\sigma(n_f,h) = \Sigma_i[N_{eff,i} - N_{eff,i}(n_f,h)]^2 \tag{15}$$

If the experimental results are perfectly accurate, we should look for n_f and h such that $\sigma = 0$. Because of the presence of the experimental error and inaccuracy, this is not possible. Instead we look for the values of n_f and h which minimize σ, and they are found by requiring

$$\frac{\partial\sigma}{\partial n_f} = 0 \tag{16}$$

$$\frac{\partial\sigma}{\partial h} = 0 \tag{17}$$

A gradient method [2] is used to solve for n_f and h from the simultaneous equations (16) and (17), and this is done by calling the subroutine GRDT. The basic idea of the gradient method is quite simple. Suppose a relief or a surface of σ is plotted as a function of (n_f,h). Let σ at a particular

point (n_f,h) be evaluated. If $\sigma = 0$, this particular point corresponds to the desired solution. If $\sigma > 0$, then a point with a smaller value of σ should be chosen. If one is standing on the relief, then the best possible move is to move in the direction of steepest descent, which is precisely the direction of the negative gradient. In GRDT, σ for a given (n_f,h), and its eight neighboring points, are calculated by repeatedly calling the subroutine ERSUM. In the process, it is necessary to solve for the effective index of refraction from (1) numerically. A quadratic interpolation algorithm expounded by Muller is used for this purpose [10]. To make use of the MULLER subroutine, the dispersion relation (1) is coded as the subroutine DISP. A valley is reached when (16) and (17) are satisfied.

4.3 Examples:

To test the accuracy of the program, two test runs have been made. The parameters of the waveguide and prism, the "observed" coupling angles and the results of the computation are listed below.

(1) Waveguide 1:

$n_s = 1.5000$, $n_c = 1.0000$, $n_p = 1.7552$, $\varepsilon = 50.0°$.

$n_f = 1.6500$, $h = 2.0000$ μm,

$\alpha = 35.95°$, $32.80°$, $28.80°$.

Computed $n_f = 1.6503$, Error = 0.018%.

Computed $h = 2.0352$ μm, Error = 1.76%.

(2) Waveguide 2:

n_s = 1.4500, n_c = 1.0000, n_p = 1.7552, ε = 50.0°.

n_f = 1.5500, h = 2.8000 μm,

α = 21.10°, 19.75°, 17.10°.

Computed n_f = 1.5495, Error = 0.03%.

Computed h = 2.7348 μm, Error = 2.3%.

The coupling angles are read and interpolated from a curve similar to Figure 3 or 4 and are accurate to ±0.1°. Comparison of the computed values for n_f and h with those assumed values shows that the results are quite good, despite of the inaccuracy in reading the coupling angles.

5.0 ATTENUATION

Although the attenuation of the guided beam can be determined by using two or three prisms [11, 12], the data so obtained is not very reliable. Instead, an optical fiber may be used to probe the intensity of the guided beam and the attenuation constant can be deduced from the measured data. Many optical films are polycrystalline in nature. The grain boundaries are distributed more-or-less uniformly throughout the film, and act as the scattering centers. Streaks of light appear when light is scattered by the scattering centers. The intensity of the scattered light is proportional to the intensity of the guided beam and can be used as a measure of the intensity of the guided beam. By plotting the intensity of scattered light as a function of position along the propagating beam, one can estimate the attenuation constant. A simple way to perform the experiment is to use a TV camera. The video image recorded by the camera can be processed electronically. A microscope objective or an optical fiber may be used to pick up the scattered light [13, 14]. Because of its size and

flexibility, an optical fiber is preferred. A fixed orientation of the fiber relative to the waveguide and a constant separation between the fiber tip and the waveguide should be maintained throughout the measurement. To avoid fluctuation or "scattering" of the data, the numerical aperture of the fiber should not be too small. The reading taken when the fiber is near the edges of the waveguide should be discarded. It is also desirable to probe the scattered light as a function of position transverse to the propagating beam and to integrate the signal so measured. Of course, such a measurement would be very time-consuming.

A Gamma Scientific Radiometer interfaced with a Hewlett-Packard 9825 Computer/Controller and various attachments are available for use at NAC. All that is needed is to construct a stable platform so that the fiber can be moved relative to the waveguide in a fixed, predetermined fashion.

6.0 EXPERIMENTAL OBSERVATIONS WITH INJECTION LASERS

Since semiconductor injection lasers are small and can be modulated directly at high frequency, they are favored in many communication and signal processing applications. The bandgap of GaAs, or ternary and quaternary compounds based on GaAs material, is such that radiation emitted from GaAs injection lasers are in the near infrared region and are invisible to human eyes. In addition, the radiation from these lasers diverges quickly. Unless a simple means is found to trace or to "see" the laser beam, it would be very difficult to align various optical components with respect to the invisible beam. Ways must also be found to collect and to collimate the beam before it diverges. Other than these two complications, experiments involving GaAs or other semiconductor lasers with near infrared (IR)

emission are essentially the same as the experiments using lasers in the visible spectra.

Two simple ways of "seeing" emission in near IR spectra are IR-phosphor plates and image converters. While the phosphor plates are easy to use, their sensitivity is rather low. Two crucial components of an image converter are a photocathode and a fluorescent screen. Electrons are ejected from the photocathode as a result of the photon bombardment. The electrons so released are accelerated toward the fluorescent screen which emits light in the visible region. Thus the IR or near IR image is converted into a visible one. Depending on the photocathodes used, the image converter may be used in different spectral regions. For example, S-1 cathodes, which are typically used in many commercially available image converters or IR viewers, are useful in the range between 0.3 to 1.2 μm with its peak response in the 0.7 to 0.9 μm range, which coincides with the emission spectra of GaAs lasers.

TV cameras equipped with Si cathodes can also be used to view near IR or IR emission. However, TV cameras are too heavy and bulky for initial alignment purpose, although they are very useful for the final viewing or detailed measurement.

The active, light-emitting area of an injection laser is quite small and generally has a rectangular shape. As a result, the beam emitted by an injection laser has an elliptical cross section with a large angle of divergence. Typically, the beam divergences are 10.° (parallel to the pn junction) x 30.° (perpendicular to the junction), i.e., 170 x 520 mrad. For comparison, it is noted that the beam divergence of a typical HeNe

laser is about 1 to 2 mrad. Since the beam diverges fast, a lens with a small F-number or a microscope objective with a large numerical aperture (N.A.) can be used to collect the beam before it diverges. The F-number of a lens is defined as the ratio of the effective focal length f to the diameter d of the aperture:

$$\text{F - number} \equiv f/d \tag{18}$$

For a microscope objective situated in the air and accepting beams within a cone of half-angle θ, the numerical aperture is

$$\text{N.A.} = \sin\theta \tag{19}$$

For lenses corrected for coma and spherical aberration and with infinite object distance, these two quantities are related:

$$\text{F - number} = \frac{1}{2\text{N.A.}} \tag{20}$$

For reference purpose and for convenience of alignment, it is convenient to superimpose a visible light with the invisible beam. A mirror and a cube beam splitter have been used for this purpose.

7.0 FABRICATION OF OPTICAL WAVEGUIDES

Many schemes are available for fabricating the waveguides. Depending on the fabrication process, the index profile in the substrate and film regions may vary considerably. A three-layer structure, with $n_f > n_s > n_c$,

is the simplest optical waveguide configuration. In most optical waveguides, the transition from the film region to the substrate region is gradual rather than abrupt. Extensive reviews of all existing fabrication processes have been reported by Chang et. al., [16], by Tien et. al., [17, 18], and by Zernike [19]. Not all waveguides are applicable in practical systems, however. Here, the fabrication of waveguides which are potentially useful in practical systems are reviewed. Specifically, techniques useful in forming solution-deposited waveguides, and waveguides based on glass and lithium niobate substrates are considered. In terms of practicality, waveguides based on GaAs should also be included in the list. As is well known, fabrication of semiconductor thin-films is a precise and complex discipline. Numerous articles and books are devoted to the subject of semiconductor thin-films in general, and GaAs or ZnO material [20-23] in particular. Therefore, optical films based on GaAs or ZnO materials are not included in the review.

7.1 Solution deposited waveguides:

Of all techniques available for producing optical films and components, techniques based on solution deposition are the simplest. Most thin-film fabrication processes have their origin in microelectronics. These techniques are eminently suited for fabricating small or miniature components. If optical films or components with large areas are needed, solution deposition or rf discharge polymerization are probably the best candidates [24-30]. The properties of polymeric thin-films have been studied by Swalen et. al., [24]. Some details of fabricating photoresists (Kodak's KPR, and Shiple AZ1350), polyurethane, epoxy, lead silica, polystyrene (PS), polymethyl

methacrylate (PMMA), styrene acrylonitrile copolymer (SAN) or combinations of PMMA and SAN have been reported [25 - 29]. The combination of PMMA and SAN has an interesting property in that the index of the film can be adjusted from 1.489 to 1.563 by properly mixing PMMA with SAN. The pertinent fabrication parameters are summarized in Table 1. The shortcomings of these films include a short life time and in some cases, attenuation is sensitive to ambient humidity [29].

After the solution is prepared, it can be applied onto a solid substrate, usually a glass slide. Uniform coating can be achieved by dipping, horizontal flow, spinning coating or "doctor blading" methods [24]. "Dipping" simply means dipping the glass slide into the solution and then withdrawing the slide from the solution with constant speed. The film thickness is controlled by the viscosity of the solution, and, to some extent, the speed of withdrawing. The slide is dried and/or baked in a horizontal position. The horizontal flow method starts with covering the slide with the solution from a syringe,the slide is then brought to a vertical position so that the excess solution is drained. The slide is returned to the horizontal position for drying and/or baking. In spin coating, the slide is placed in a spinner. After the slide is covered with the solution, it is spun with a specific speed and for a specific duration so as to achieve a given thickness. Since the speed and duration of spin can be controlled, in addition to the density and the viscosity of the solution, the films so obtained are quite uniform. In the "doctor blading" method, a knife edge is used to spread the solution along the surface of the slide.

7.2 Glass waveguides:

Most optical systems used in communication or sensor applications will require optical fibers as their transmission media. At present, optical fibers are made of glass or quartz and have indices of refraction in the range of 1.5 to 1.6. Since the IO components are a part of the communication or sensor system, it is necessary to interface the IO components to the optical fibers. To reduce the reflection loss at the interfaces, the indices of the glass fibers and the IO components should be matched as closely as practical. Waveguides based on glass or quartz substrate are the natural choice in those applications. R.F. sputtering [31 - 38], chemical vapor deposition (CVD) [39], vacuum or electron beam deposition [35, 40], ion implantation [41 - 43], and ion exchange [44 - 52] methods have been used in forming waveguides on various glass slides. Thermal evaporation in vacuum is probably the simplest way of depositing thin films onto a substrate. However, films produced by thermal evaporation tend to be quite lossy. If the electron-beam evaporation process is used, films 2 to 4 μm thick may be obtained with an attenuation slightly larger than 1.0 dB/cm [40] which is comparable to the waveguides made by sputtering processes.

Films of good quality with various compositions may be produced by the r.f. sputtering process. The composition of the gases in which sputtering is performed, the rf power and duration of sputtering can be controlled with ease. The gas pressure and the temperature of the substrate can also be adjusted to some extent. These fabrication parameters can be varied to form films having the desired composition and thickness. Obviously, the film thickness is directly proportional to the duration of sputtering. The

rf power can be varied to tailor the index of sputtered film, and the stoichiometry of the film can be compensated by admitting various gases in the various stages of sputtering [33, 34]. The sputtering parameters and the properties of the films so obtained are summarized in Table 2.

The refractive index of a film is a function of the density and the electronic polarizability of the constituent species, and is described by the Clausius-Mossotti relation [53]. If the density of the material is increased, so is the index of refraction. More importantly, if the composition of the material is changed so that species with small electronic polarizability are replaced by species with large electronic polarizability, the index of refraction is also increased. In forming waveguides by solution deposition, thermal evaporation or r.f. sputtering, layers of material with higher index are deposited onto substrates, and the resulting index profiles are more-or-less abrupt. In the ion exchange process, however, an optical waveguide is formed when ions with small polarizability near the substrate surface are replaced by ions with larger polarizability, and the index profile of an ion-exchanged waveguide changes gradually from the surface (i.e., the "film" region) to the substrate region. Ion exchange processes can be used to form waveguides in glass, lithium niobate or other substrates. In this section, the discussion is restricted to glass or quartz. Typically, a glass slide is immersed at elevated temperature in molten salts containing the ions to be exchanged. Compounds such as KNO_3 , $TlNO_3$, and $NaNO_3$ [44], or $AgNO_3$ [45-47, 50],or $AgNO_3$ and $NaNO_3$ [51], or a eutectic melt of Li_2SO_4 and K_2SO_4 [48] have been used in conjunction with various glasses. Alternatively, a solid silver film or a vapor stream of silver, produced

by thermal evaporation, may be used instead of melts [49, 52]. The exchange process can be done with or without the assistance of an electric field. In the presence of an electric field, the speed of ion exchange is increased, and processing time can be reduced. Electric fields can also be used to make the index profile more abrupt and to move the peak of the index profile to the interior region of the substrate. By diffusing Ag^+, Tl^+ and K^+ ions into the glass to replace Na^+ and Li^+ ions, the index of the diffused region will be higher than the index of the undiffused region. Masks with windows or apertures can be placed on the glass surface so that ion exchange is restricted to the selected regions. In this fashion, strip waveguides can be formed [46]. The fabrication parameters of ion exchange process are tabulated in Table 3.

7.3 Lithium niobate waveguides:

Since lithium niobate and lithium tantalate are highly transparent and have large electro-optic coefficients, they are commonly used waveguide materials. In particular, lithium niobate waveguides have been used to demonstrate the feasibility of many device concepts and practical systems. The epitaxial growth by melting method has been used to grow a solid solution of $(LiNbO_3)_\alpha(LiTaO_3)_{1-\alpha}$ onto $LiTaO_3$ substrate [54]. A guiding layer can also be formed by thermally diffusing, or diffusing under electric field, metals like Cu, Al, Ge, Cr, Fe, and Nb into $LiTaO_3$ [55 - 57], or by releasing Li_2O from the surface of $LiNbO_3$ or $LiTaO_3$ [58,59]. By far the most popular method is to deposit a layer of transition metal like Ti, V or Ni, on the surface of $LiNbO_3$ and to diffuse these elements into the

substrate. This is known as the in-diffusion process [60]. Of the transition metals mentioned, Ti is the most popular element used, and it leads to the well known Ti:$LiNbO_3$ waveguides [60 - 64]. In the diffusion process, the temperature of the substrate has to be raised, Li_2O is released from the surface resulting in an unwanted out-diffused waveguide at the surface of the substrate. Considerable effort was devoted to the elimination of the out-diffused layer [65 - 70]. The simplest way of suppressing the out-diffused waveguide layer is to add water vapor in the diffusion gas [70]. Table 4 lists most pertinent parameters in forming in-diffused waveguides.

Ion exchange methods have also been used to form optical waveguides on $LiNbO_3$ and $LiTaO_3$ [71, 72]. By exchanging Li^+ ions or the vacant sites for Li^+ ions with metallic ions, optical waveguides can also be formed in $LiNbO_3$ of $LiTaO_3$. By placing polished x-cut plate of $LiNbO_3$ in molten $AgNO_3$ at 360°C for 3 to 15 hours, waveguides capable of supporting 1 to 3 TE modes were obtained by Shah [71]. The attenuation constant was measured with an optical fiber probe to be 6 dB/cm. The increase in the extraordinary index of refraction is quite large, ($\Delta n_e \simeq 0.12$). But the change in the ordinary index of refraction is insignificant, and no TM modes were observed. Experiments were also performed showing that the electro-optic coefficients of $LiNbO_3$ are not significantly affected by the ion exchange process. Y-cut $LiNbO_3$ or $LiTaO_3$ samples were also placed in $AgNO_3$ melt for 24 hours, no waveguide layer was formed, however. Additional work reported by Jackel [72] showed that the loss can be reduced to the 0.8 to 2.0 dB/cm region. Larger change in the extraordinary index of refraction has been obtained when the Li^+ ions are exchanged with Tl^+ ions in molten $TlNO_3$.

8.0 CONCLUSION

With the introduction of integrated optics, a new class of optical components and systems emerge. Thin-film optical waveguides are the building blocks of these systems. Methods for fabricating, and experimental and numerical techniques for characterizing these waveguides were studied. Techniques useful for performing experiments in visible and infrared spectra were discussed. This study serves as a brief introduction to a new horizon in command, control and communication systems which has particular utility in avionics instrumentation.

ACKNOWLEDGEMENT

The author wishes to acknowledge the contribution of Drs. K. J. Jones and C. T. Simpson of Naval Avionics Center. Much of the work reported here was performed jointly with them. He is also grateful to Messrs. T. Corbin and D. Perin for their technical support and assistance.

REFERENCES:

1. P. K. Jien, "Light waves in thin-films and integrated optics," Appl. Optics, Vol. 10, pp. 2395 - 2413, (1971).

2. R. Ulrich and R. Torge, "Measurement of thin film parameters with a prism coupler," Appl. Optics, Vol. 12, pp. 2901 - 2908, (1973).

3. E. R. Schumacher, "Defect-free edge polishing of lithium niobate and other optical crystals", NOSC TR 480, Optics Laboratory, Naval Ocean Systems Center, San Diego, CA 92152, (1980).

4. H. Kogelnik, "Imaging of optical modes - resonators with internal lenses," Bell Syst. Tech. J., Vol. 44, pp. 455 - 494, (1963).

5. L. P. Boivin, "Thin-film laser-to-fiber coupler", Appl. Opt., Vol. 13, pp, 391 - 395, (1974).

6. R. K. Winn, J. H. Harris, "Coupling from mode to single-mode linear waveguides using horn-shaped structures", IEEE Trans. on Microwave Theory and Techniques, Vol. MTT-23, pp. 92 - 97, (1975).

7. A. R. Nelson, "Coupling optical waveguides by tapers", Appl. Opt., Vol. 14, pp. 3012 - 3015, (1975).

8. W. K. Burns, A. F. Milton, and A. B. Lee, "Optical waveguide parabolic coupling horns", Appl. Phys. Lett., Vol. 33, pp. 28 - 30, (1977).

9. A. F. Milton, W. K. Burns, "Mode coupling in optical waveguide horns", IEEE J. of Quant. Electronics, Vol. QE-13, pp. 828 - 835, (1977).

10. S. D. Conte, C. de Boor, "Elementary Numerical Analysis", McGraw-Hill Books Co., second ed., p. 74, (1972).

11. H. P. Weber, F. A. Dunn, W. N. Leibolt, "Loss measurements in thin-film optical waveguides", Appl. Optics, Vol. 4, pp. 755 - 757, (1973).

12. Y. H. Won, P. C. Jauss, G. H. Chartier, "Three-prism loss measurement of optical waveguides," Appl. Phys. Lett., Vol. 37, pp. 269 - 271, (1980).

13. H. Mori, M. Itakura, "The scattering centers in dielectric thin film optical waveguides," Japan J. of Appl. Phys., Vol. 14, pp. 1917 - 1924, (1975).

14. J. E. Goell, R. D. Standley, "Integrated optical circuits", Proc. IEEE, vol. 58, pp. 1504 - 1512, (1970).

15. M. Born, E. Wolf, "Principles of Optics", 6th Edition, Sec. 4.8.2, Pergamnon Press, (1980).

16. W. S. C. Chang, M. W. Muller, F. J. Rosenbaum, "Integrated Optics", in "Laser Applications", Vol. 2, Academic Press, New York, (1974).

17. P. K. Tien, A. A. Ballman, "Research in optical films for the applications of integrated optics", J. Vac. Sci. Technol., vol. 12, pp. 892 - 904, (1975).

18. P. K. Tien, "Integrated optics and new wave phenomena in optical waveguides", Rev. Mod. Phys., Vol. 49, pp. 361 - 420, (1977).

19. F. Zernike, "Fabrication and measurement of passive components", in "Integrated Optics", edited by T. Tamir, Springer-Verlag, New York, (1975).

20. V. Evtuhov, A. Yariv, "GaAs and GaAlAs devices for integrated optics," IEEE Trans. on Microwave Theory and Techniques, Vol. MTT-23, pp. 44 - 57, (1975).

21. E. Garmire, "Semiconductor components for monolithic applications", in "Integrated Optics", edited by T. Tamir, Springer-Verlag, New York, (1975).

22. H. Kressel, J. K. Butler, "Semiconductor Lasers and Heterojunction LEDs", Academic Press, New York, (1977).

23. H. C. Casey, Jr., M. B. Panish, "Heterostructure Lasers, Part B: Materials and Operating Characteristics", Academic Press, New York, (1978).

24. J. D. Swalen, R. Santo, M. Tacke, J. Fischer, "Properties of polymeric thin films by integrated optical techniques", IBM J. of Research and Development, Vol. 21, pp. 168 - 175, (1977).

25. D. B. Ostrowsky, A. Jacques, "Formation of optical waveguides in photoresist films," Appl. Phys. Lett., Vol. 18, pp. 556 - 557, (1971).

26. R. Ulrich, H. P. Weber, "Solution deposited thin films as passive and active light-guides", Appl. Optics, Vol. 11, pp. 428 - 434, (1972).

27. V. Ramamswamy, H. P. Weber, "Low-loss polymer films with adjustable refractive index", Appl. Optics, Vol. 12, pp. 1581 - 1583, (1973).

28. D. G. Dalgoutte, C. D. W. Wilkinson, "Thin grating couplers for integrated optics: an experimental and theoretical study," Appl. Optics, Vol. 14, pp. 2980 - 2998, (1975).

29. J. M. Mahoney, T. E. Batchman, "Polystyrene solution deposited optical waveguides and couplers," Proc. IREE (Australia), pp. 369 - 371, (1975).

30. P. K. Tien, G. Smolinsky, R. J. Martin, "Thin organosilicon films for integrated optics", Appl. Opt., Vol. 11, pp. 637 - 642, (1972).

31. J. E. Goell, R. D. Standley, "Sputtered glass waveguide for integrated optical circuits", Bell Syst. Tech. J., Vol. 48, pp. 3445 - 3448, (1969).

32. M. L. Dakes, L. Kuhn, P. F. Heidrich, B. A. Scott, "Grating coupler for efficient excitation of optical guided waves in thin films", Appl. Phys. Lett., Vol. 16, pp. 523 - 525, (1970).

33. C. W. Pitt, "Sputtered glass optical waveguides", Electron. Lett., Vol. 9, pp. 401 - 402, (1973).

34. C. W. Pitt, F. R. Gfeller, R. J. Stevens, "R.F. sputtered thin-films for integrated optical components", Solid Thin Films, Vol. 26, pp. 25 - 51, (1975).

35. P. K. Tien, R. Ulrich, R. J. Martin, "Modes of propagating light waves in thin deposited semiconductor", Appl. Phys. Lett., Vol. 14, pp. 291 - 294, (1969).

36. R. H. Deitch, E. J. West, T. G. Giallorenzi, J. F. Weller, "Sputtered thin films for integrated optics", Appl. Opt., Vol. 13, pp. 712 - 715, (1974).

37. J. E. Goell, "Barium silicate films for integrated optical circuits," Appl. Opt., Vol. 12, pp. 737 - 742, (1972).

38. M. Fujimor, A. Okamoto, Y. Nishimura, "Tantalum pentoxide thin films for light guide", Fujitsu Sci. & Tech. J., Vol. 8, pp. 177 - 189, (1972).

39. M. J. Rand, R. D. Standley, "Silicon oxynitride films on fused silica for optical waveguides," Appl. Opt. Vol. 11, pp. 2482 - 2488, (1972).

40. T. R. Kersten, W. Rauscher, "A low loss thin film optical waveguide for integrated optics made by vacuum evaporation", Optics Comm., Vol. 13, pp. 189 - 191, (1975).

41. R. E. Schineller, R. P. Flam, D. W. Wilmot, "Optical waveguides formed by proton irradiation of fused silica", J. Opt. Soc. Am., Vol. 58, pp. 1171 - 1176, (1968).

42. R. D. Standley, W. M. Gibson, J. W. Rodgers, "Properties of ion-bombarded fused quartz for integrated optics", Appl. Opt., Vol. 11, pp. 1313 - 1316, (1972).

43. J. E. Goell, R. D. Standley, W. M. Gibson, J. W. Rodgers, "Ion bombardment fabrication of optical waveguides using electron resist masks," Appl. Phys. Lett., Vol. 21, pp. 72 - 73, (1972).

44. T. Izawa, H. Nakagome, "Optical waveguide formed by electrically induced migration of ions in glass plates", Appl. Phys. Lett., Vol. 12, pp. 584 - 586, (1972).

45. R. G. Giallorenzi, E. J. West, R. Gunther, R. A. Andrews, "Optical waveguides formed by the thermal migration of ions in glasses", Appl. Optics, Vol. 12, pp. 1240 - 1245, (1973).

46. J. G. Gallagher, R. M. De La Rue, "Single mode strip optical waveguides formed by silver ion exchange", Electron. Lett., Vol. 12, pp. 397 - 398, (1976).

47. G. Stewart, "Planar optical waveguides formed by silver ion migration in glass, " IEEE J. Quantum Electron., Vol. QE-13, pp. 192 - 200, (1977).

48. G. H. Chariter, P. Jaussaud, A. D. De Oliveriora, O. Parriaux, "Fast fabrication method for thick and highly multimode optical waveguides," Electron. Lett., Vol. 13, pp. 763 - 764, (1977).

49. G. H. Chariter, P. Jaussaud, A. D. De Oliveriora, O. Parriaux, "Optical waveguides formed by electric field controlled ion exchange in glass," Electron. Lett., Vol. 14, pp. 132 - 134, (1978).

50. C. A. Millar, R. H. Hutchins, "Manufacturing tolerances of silver-sodium ion-exchanged planar optical waveguides," J. Phys., D: Appl. Phys. Vol. 11, pp. 1567 - 1576, (1978).

51. T. G. Steward, P. J. R. Laybourn, "Fabrication of ion-exchanged waveguides from dilute silver nitrate melts", IEEE J. Quantum Electron., Vol. QE-14, (1978).

52. C. W. Pitt, A. A. Stride, R. I. Trigle, "Low temperature diffusion process for fabricating optical waveguides in glass," Electron. Lett., Vol. 16, pp. 701 - 703, (1980).

53. C. Kittel, "Introduction to Solid State Physics", Wiley & Sons, Inc., New York, (1968), Chapter 12.

54. P. K. Tien, Riva-Sanseverino, R. Martin, "Optical waveguide modes in single-crystalline $LiNbO_3$-$LiTaO_3$ solid solution films," Appl. Phys., Vol. 24, pp. 503 - 506, (1974).

55. J. M. Hammer, W. Phillips, "Low-loss single mode optical waveguides and efficient high-speed modulators of $LiNb_xTa_{1-x}O_3$ on $LiTaO_3$," Appl. Phys. Vol. 24, pp. 545 - 547, (1974).

56. J. Noda, T. Saku, N. Uchida, "Fabrication of optical waveguiding layer in $LiTaO_3$ by Cu diffusion," Appl. Phys. Lett., Vol. 25, pp. 308 - 310, (1974).

57. R. D. Standley, V. Ramaswamy, "Nb-diffused $LiTaO_3$ optical waveguides: Planar and embedded strip guides", Appl. Phys. Lett., Vol. 25, pp. 711 - 713, (1974).

58. I. P. Kaminow, J. R. Carruthers, "Optical waveguiding layers in $LiNbO_3$ and $LiTaO_3$", Appl. Phys. Lett., Vol. 22, pp. 326 - 328, (1973).

59. J. R. Carruthers, I. P. Kaminow, L. W. Stulz, "Diffusion kinetics and optical waveguiding properties of outdiffused layers in lithium niobate and lithium tantalate", Appl. Opt., Vol. 13, pp. 2333 - 2342, (1974).

60. R. V. Schmidt, I. P. Kaminow, "Metal-diffused optical waveguides in $LiNbO_3$," Appl. Phys. Lett., Vol. 25, pp. 458 - 460, (1974).

61. J. Noda, M. Fukuma, S. Saito, "Effect of Mg ion diffusion on Ti-diffused $LiNbO_3$ waveguides", J. Appl. Phys., Vol. 49, pp. 3150 - 3154, (1978).

62. M. Fukuma, J. Noda, H. Iwasaki, "Optical properties in titanium diffused $LiNbO_3$ strip waveguides," J. Appl. Phys., Vol. 49, pp. 3693 - 3698, (1978).

63. J. Noda, S. Zembutsu, S. Fukunishi, N. Uchida, "Strip loaded waveguide formed in a graded index $LiNbO_3$ planar waveguide," Appl. Opt., Vol. 17, pp. 1953 - 1958, (1978).

64. L. W. Stulz, "Titanium in-diffused $LiNbO_3$ optical waveguide fabrication," Appl. Opt.,Vol. 18, pp. 2041 - 2044, (1979).

65. T. R. Ranganath, S. Wang, "Suppression of Li_2O out-diffusion from Ti-diffused $LiNbO_3$ optical waveguides," Appl. Phys. Lett., Vol. 30, pp. 376 - 379, (1977).

66. B. U. Chen, A. C. Pastor, "Elimination of Li_2O out-diffusion waveguide in $LiNbO_3$ and $LiTaO_3$," Appl. Phys. Lett., Vol. 30, pp. 570 - 571, (1977).

67. S. Miyazawa, R. Guglielmi, A. Carenco, "A simple technique for suppressing Li_2O out-diffusion in Ti: $LiNbO_3$ optical waveguide," Appl. Phys. Lett., Vol. 31, pp. 742 - 744, (1977).

68. W. K. Burns, C. H. Bulmer, E. J. West, "Application of Li_2O compensation techniques to Ti-diffused $LiNbO_3$ planar and channel waveguides," Appl. Phys. Lett., Vol. 33, pp. 70 - 72, (1978).

69. R. J. Esdaile, "Closed-tube control of out-diffusion during fabrication of optical waveguides in $LiNbO_3$," Appl. Phys. Lett., Vol. 33, pp. 733 - 734, (1978).

70. J. L. Jackel, V. Ramaswamy, S. P. Lyman, "Elimination of out-diffused surface guiding in titanium-diffused $LiNbO_3$," Appl. Phys. Lett., Vol. 38, pp. 509 - 511, (1981).

71. M. L. Shah, "Optical waveguides in $LiNbO_3$ by ion exchange technique," Appl. Phys. Lett., Vol. 26, pp. 652 - 653, (1975).

72. J. L. Jackel, "Ion exchange for optical waveguides in $LiNbO_3$ and $LiTaO_3$," paper WB4, Topical Meeting on Integrated and Guided-wave Optics, Incline Village, NV, (Jan. 1980). Also, "High Δn optical waveguides in $LiNbO_3$: thallium-lithium ion exchange", Appl. Phys. Lett., Vol. 37, pp. 739 - 741, (1980).

APPENDIX - LISTING OF A COMPUTER PROGRAM

In this Appendix, the program MAIN and the subroutines used to compute or estimate the refractive index n_f and the thickness h of the film from the measured coupling angles are listed. These programs, written in the standard Fortran language, have been tested as described in the main text of this report.

```
      program main(input,output)
      common /d1/ lambda,nefms(20), m(20),nss,ncs,mrho,nlines
      common /d3/ neft(20)
      real ns,nc,nf,np,lambda
      real nss,ncs,nfs,kw
      dimension theta(20), m(20)
      real neft(20), nefm(20), nefms(20)
      external ersum
c     open(1,file='mdata', status='old')
c     rewind 1
      read(5,180)ns,nc,np,lambda,epsm,mrho
 180  format(5(f8.4,2x),i2)
      anp2=np*np
      nss=ns*ns
      ncs=nc*nc
      pi=3.141592654
      if(mrho .eq. 0) write (6,190)
      if(mrho .eq. 1) write (6,191)
 190  format(3x,'TE MODES' )
 191  format(3x,'TM MODES' )
      write(6,183)ns,nc,np,epsm,lambda
 183  format(2x,'ns= 'f8.4,' nc= 'f8.4,' np= 'f8.4, ' angle of prism = '
     1 f8.4,3x,' lambda= 'f8.4)
      epsmr=epsm*pi/180.
      do 184 i=1,20
      read(5,*,end=299) m(i),theta(i)
 184  nlines=i
c
      write(6,185)
 185  format(3x,'More than 20 m-lines ? ')
      goto 999
c
 299  do 298 i=1,nlines
 298  write(6,186) m(i), theta(i)
 186  format(3x,i2,f8.4, '  degrees')
```

```
c
      do 220 ie=1,nlines
      thetar=theta(ie)*pi/180.
      nefm(ie)=sin(thetar)*cos(epsmr)+(sin(epsmr)*sqrt(anp2-sin(thetar)
     1 *sin(thetar)))
      nefms(ie)=nefm(ie)*nefm(ie)
      neft(ie)=nefm(ie)
      write(6,215) ie,theta(ie),nefm(ie)
 215  format(3x,i2,'-th coupling angle = 'f8.3,3x,'N eff = 'f8.4)
 220  continue
c     if(nlines .gt. 2) goto 500
      nf=1.048*amax1(nefm(1), nefm(2))
      nfs=nf*nf
      fts=1.
      ftc=1.
      do 300 iq=1,15
      if(mrho .eq. 1) ftc=(nfs/ncs)*(nfs/ncs)
      if(mrho .eq. 1) fts=(nfs/nss)*(nfs/nss)
      phis=atan(sqrt(fts*(nefms(1) - nss)/(nfs - nefms(1))))
      phic=atan(sqrt(ftc*(nefms(1) - ncs)/(nfs - nefms(1))))
      psi1=m(1)*pi+phis+phic
      phis=atan(sqrt(fts*(nefms(2) - nss)/(nfs - nefms(2))))
      phic=atan(sqrt(ftc*(nefms(2) - ncs)/(nfs - nefms(2))))
      psi2=m(2)*pi+phis+phic
      f=(nefms(2)*psi1*psi1-nefms(1)*psi2*psi2)/(psi1*psi1 -psi2*psi2)
      test=abs((nfs-f)/nfs)
      ff=sqrt(f)
      write(6,315)ff,nf,test
 315  format(3x,'nf= 'e14.6,3x,'last nf= 'e14.6,'test= ' e14.6)
      if(test .lt. 0.000001) goto 400
      nf=ff
      nfs=f
 300  continue
      write(6,320)
 320  format(3x,'*** 2 m-lines, not converging in 15 iterations.***')
      goto 999
 400  w1=lambda*psi1/(2.*pi*sqrt(nfs-nefms(1)))
      w2=lambda*psi2/(2.*pi*sqrt(nfs-nefms(2)))
      write(6,316)nf,w1, w2
 316  format(3x,'nf= 'f8.4,3x,'w1= 'f10.4,3x,'w2= 'f10.4,3x,' microns')
      if(nlines .eq. 2) goto 999
 500  kw=2.*pi*w1/lambda
      hx=1. e-8
      hy=1. e -8
      epsiln=1. e-6
      call grdt(ersum,hx,hy,nf,kw,epsiln)
      w=kw*lambda/(2.*pi)
      write(6,349)nf,w
 349  format(3x,'nf= 'f8.4,3x,'w= 'f10.4,3x,' microns')
 999  stop
      end
```

```
      subroutine disp(aneffs, dispft)
      common /d1/ lambda,nefms(20), m(20),nss,ncs,mrho,nlines
      common /d2/ nfx,wy,mij,factor
      real nf,nfx,nss,ncs,nfs
      dimension m(20)
      nfs=nfx*nfx
      pi=3.141592654
      anefs=aneffs/factor
      fts=1.
      ftc=1.
      if(mrho .eq. 1) ftc=(nfs/ncs)*(nfs/ncs)
      if(mrho .eq. 1) fts=(nfs/nss)*(nfs/nss)
      phis=atan(sqrt(fts*(anefs-nss)/(nfs -anefs)))
      phic=atan(sqrt(ftc*(anefs-ncs)/(nfs -anefs)))
      psi=mij*pi+phis+phic
      dispft=wy*sqrt(nfs-anefs)- psi
c     write(6,980)nfx,wy,aneffs,dispft
 980  format(1x,'disp',4(e14.6,1x))
      return
      end
c
```

```
      function ersum(rtn,rtw)
      common /d1/ lambda,nefms(20), m(20),nss,ncs,mrho,nlines
      common /d2/ nfx,wy,mij,factor
      common /d3/ neft(20)
      real neft(20),nefmij
      real lambda, nefms(20),nss,ncs,nfx
      dimension m(20)
      complex rtsf(4)
      external disp
      logical fnreal
      real nfse
      kn=0
      n=1
      ep1=1. e-6
      ep2=1. e-6
      fnreal=.true.
      maxit=100
      ersum=0.
      factor=1. e+4
      nfx=rtn
      wy=rtw
      nfse=nfx*nfx
      ijn=nss*factor
      ijm=nfse*factor -1
      do 100 ij=1,nlines
      ijkm=0
      mij=m(ij)
      nefmij=sqrt(nefms(ij))
      rts=(neft(ij))*(neft(ij))
      rtsf(1)=rts*factor
210   call muller(kn,n,rtsf,maxit,ep1,ep2,disp,fnreal)
      call disp(rtsf(1), dispft)
      rts=real(rtsf(1)/factor)
      if(rts .gt. nss  .and. rts .lt. nfse) goto 220
      if(ijkm .gt. 0) goto 250
      ijkm=1
      ansf=nss*factor
      call disp(ansf,ftr1)
      do 240 ijk=ijn, ijm,2
      ansf=ijk
      call disp(ansf,ftr)
      if(ftr*ftr1 .ge. 0.) goto 249
      rtsf(1)= ansf
      goto 210
249   ftr1=ftr
250   write(6,251)ijk,rtn,rtw,ansf,ftr
251   format(1x,'ersum 'i3,2(1x,f10.7),1x,'ansf= 'e14.6,' ftr= 'e14.6,
     1/ 4x,'but, no root is found.' )
240   continue
220   neft(ij)=sqrt(rts)
      ijkm=0
      ersum=ersum + (rts -nefmij)*(rts-nefmij)
      write(6,998)ij,rtn,rtw,rts,dispft
998   format(1x,'ersum 'i3,2(1x,f10.7),1x,'rts= 'e14.6,1x,'disp= 'e14.6)
100   continue
      return
      end
```

```
      subroutine grdt(fn,hx,hy,rtx,rty,epsiln)
      external fn
      noit=0
100   noit=noit+1
      f0=fn(rtx,rty)
      f1=fn(rtx+hx, rty)
      f2=fn(rtx,rty+hy)
      f3=fn(rtx-hx, rty)
      f4=fn(rtx,rty-hy)
      f5=fn(rtx+hx, rty+hy)
      f6=fn(rtx-hx,rty+hy)
      f7=fn(rtx-hx, rty-hy)
      f8=fn(rtx+hx, rty-hy)
      sx=(f1-f3)/(2.*hx)
      sy=(f2-f4)/(2.*hy)
      sxx=(f1 -2.*f0 +f3)/(hx*hx)
      syy=(f2 -2.*f0 + f4)/(hy*hy)
      sxy=(f5 - f6 -f8 + f7)/(4.*hx*hy)
      write(6,141)f0, f1,f2,f3,f4,f5,f6,f7,f8,sx,sy,sxx,syy,sxy
141   format(3x,'grdt f0, f1,f2,f3,f4 f5,f6,f7,f8 sx,sy sxx,syy,sxy '
     1/3x,e12.4,/4(3x,e12.4)/4(3x,e12.4)/2(3x,e12.4)
     2/3(3x,e12.4))
      det=sxx*syy -sxy*sxy
      rtx1=rtx + (sy*sxy -sx*syy)/det
      rty1=rty + (sx*syy -sy*sxx)/det
      write(6,142)det, rtx,rty,rtx1,rty1
142   format(3x,'det= 'e14.6,
     1/3x,'rts,rty= '2(3x,e14.6) /3x,'rtx1,rty1= '2(3x,e14.6))
      error=sqrt((rtx1-rtx)*(rtx1-rtx) +(rty1-rty)*(rty1-rty))
      error=error/sqrt(rtx*rtx +rty*rty)
      write(6,998)noit
      if(error .le. epsiln) goto 110
      rtx=rtx1
      rty=rty1
998   format(3x,'grdt noit= 'i4)
      noit=noit+1
      if(noit .gt. 20) write(6,120)
      if(noit .le. 20) goto 100
120   format(3x,'more than 20 iteration.')
110   return
      end
1     32.8
2     28.8
```

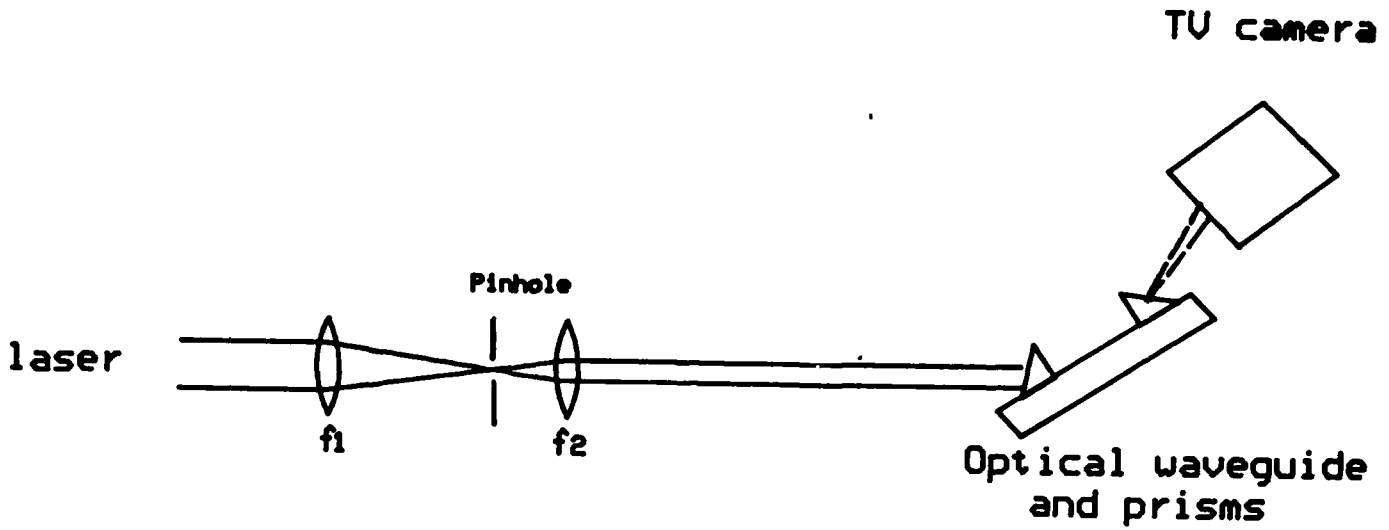

Figure 1 Setup for prism coupling experiment

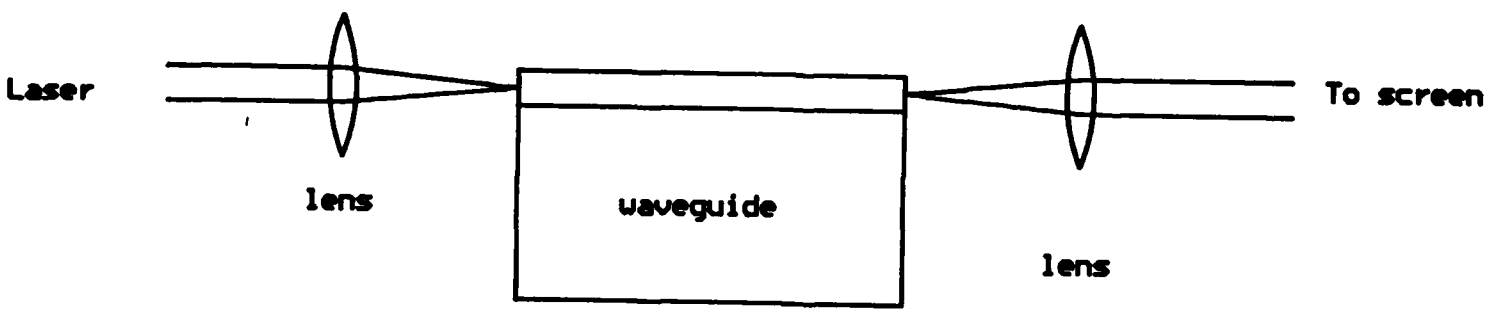

Figure 2 End Fire Coupling

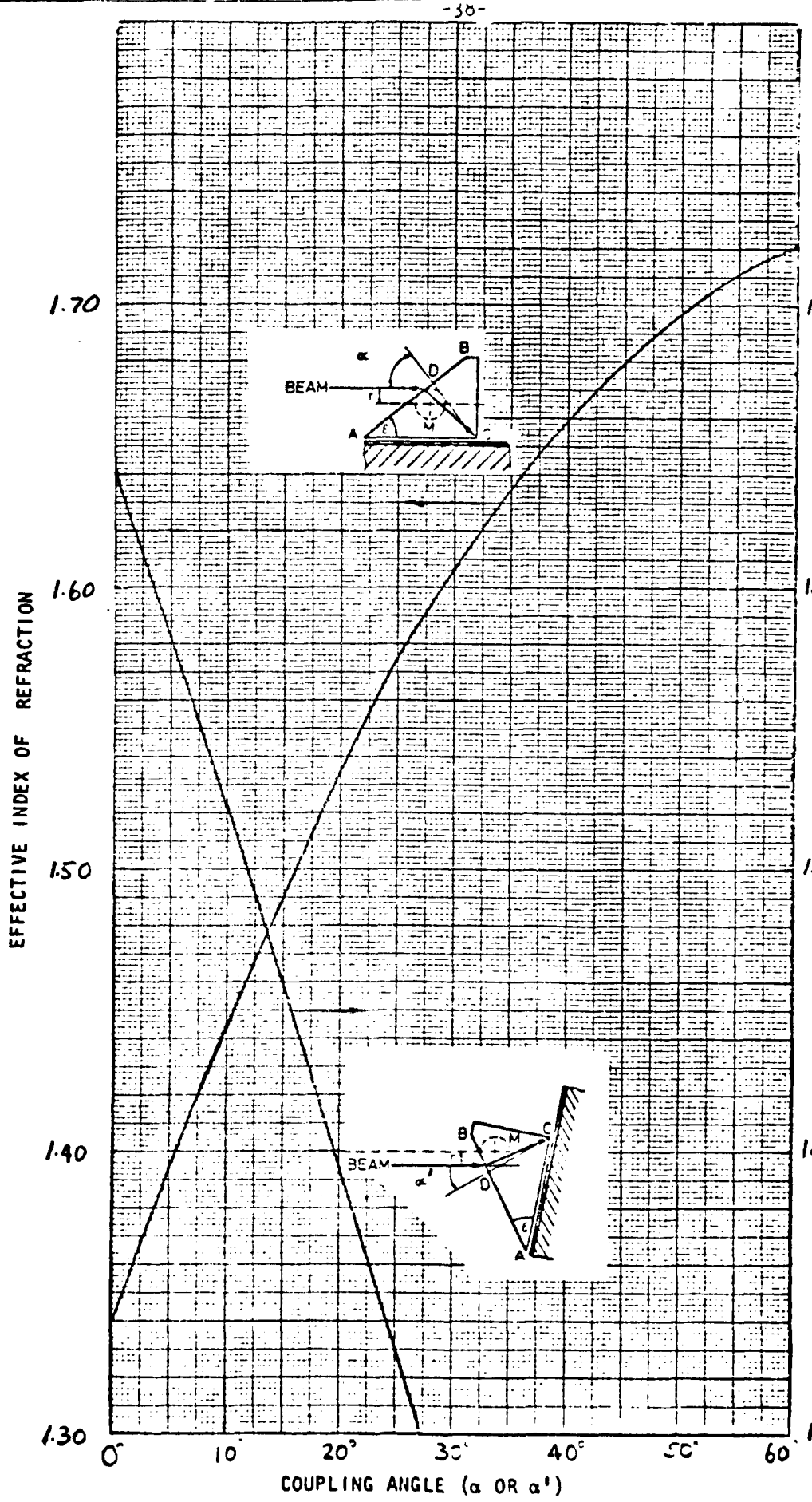

Figure 3 Effective refractive index vs coupling angle for a flint glass prism.

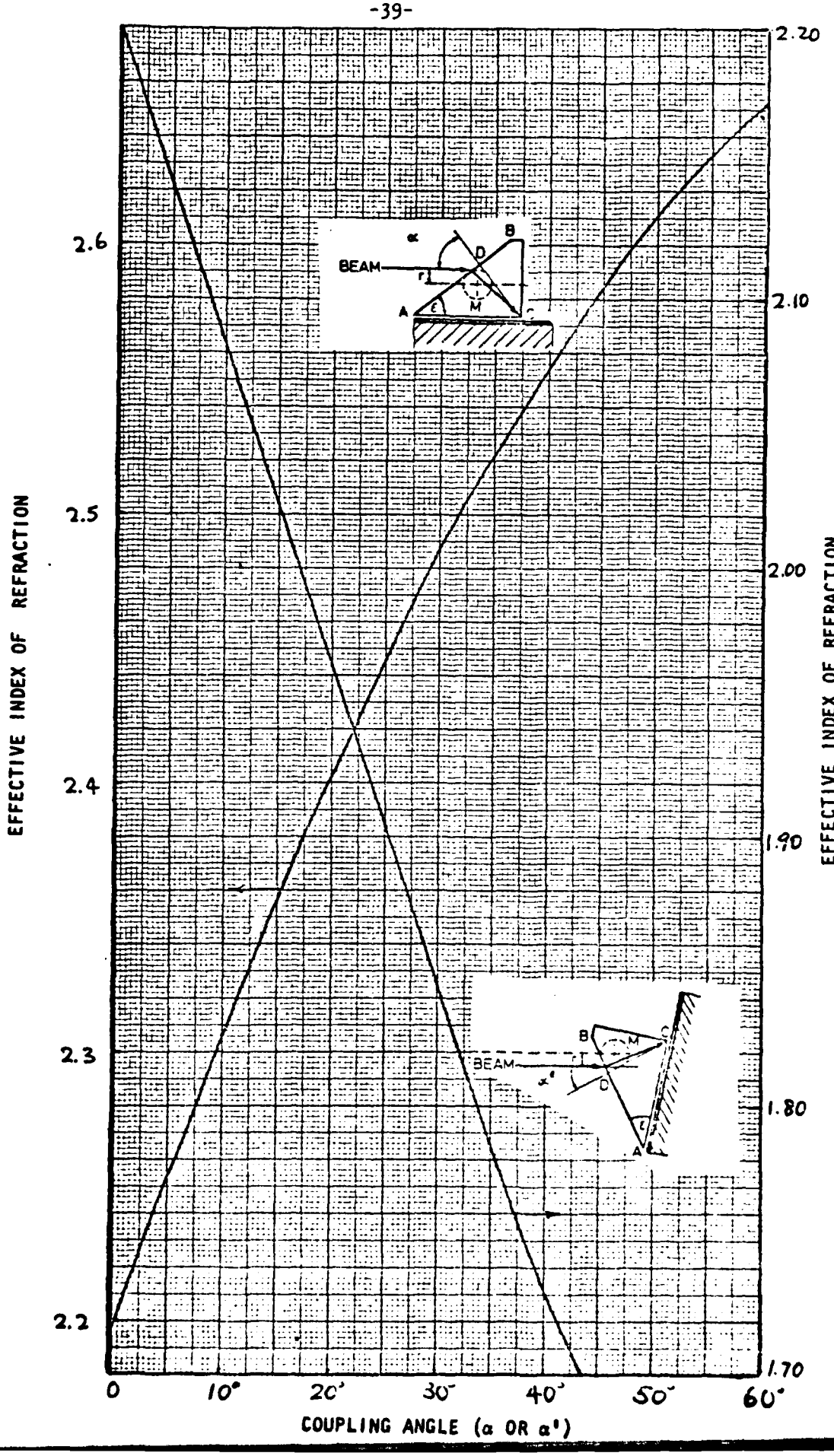

Figure 4 Effective refractive index vs coupling angle for a rutile prism.

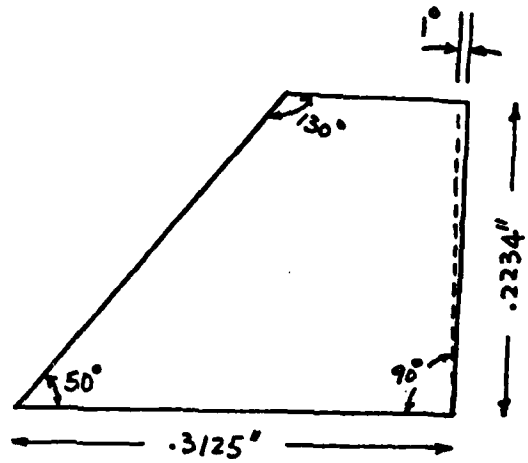

Thickness: 0.4375"
For rutile prisms, the optical axis should be perpendicular to the paper.

Figure 5 A possible design for a prism.

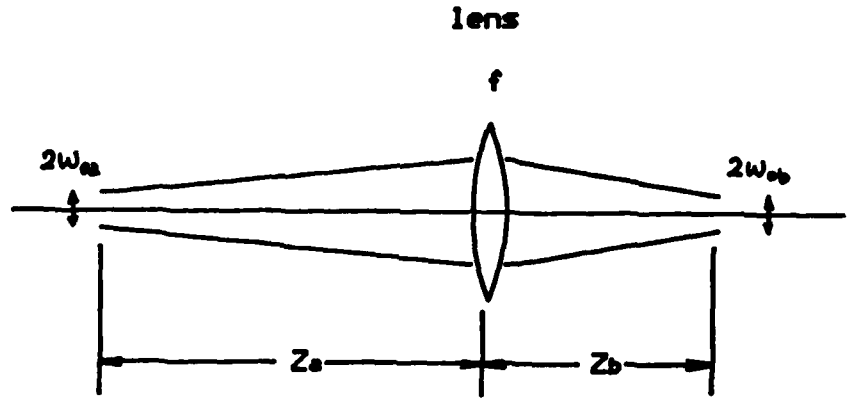

Figure 6 Transformation of Gaussian beam by a lens

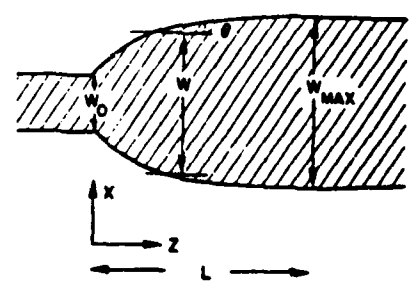

Figure 7 Top view of a parabolic waveguide horn (after Burns, et. al.)

TABLE 1. Solution Deposited Waveguides

Film Material	Polyurethane		Epoxy Resins	Lead-Silica	Polymethyl methacrylate (PMMA) and styrene-acrylonitrile copolymer (SAN)	Polystyrene (PS)	Photoresists		
Compound A	Epoxylite 9653-1 A	Midland LX500 7-C-23	Araldite 509	Emulsitone 112, A	Dupont Elvacite 2009 (PMMA)	Polymerized polystyrene	Shipley AZ-1350	Shipley AZ-1350	Kodak KPR
Compound B	Epoxylite 9653-1 B	Midland LX500 10-C-32	Araldite 951	Emulsitone 112, B	Union Carbide, RND 4500 (SAN)		-	-	-
Thinner C or Solvent	Midland 66-C-20	66-C-20	66-C-20	Methanol	Methilisobutylketone (MIBK) with .01% GE silicon oil (electronic grade) SSBI (50)	Toluene just below boiling point (~100°C)	-	-	-
Thinner D	-	-	Ethanol	-	-	-	-	-	-
Ratio A:B:C:D	1:1:8	3:1:15	7:1:16:72	1:1:2	SAN, PMMA any proportion, solvent 10% wt.	1 g. of PS in 50 c.c. of solvent	-	-	-
Drying Environment	air	air	air	air	Nitrogen	air	air	air	air
Drying Time	30 min.	60 min.	60 min.	60 min.	30 min.	15 min.		5 min.	60 min.
Baking Temperature	65°C	65°C	100°C	60°C	42°C 80°C			60°C	95°C
Baking Time	60 min.	120 min.	120 min.	10 min.	73 hrs. 24 hrs.			60 min.	5 min.
Typical Thickness	0.8 μm	2.6 μm	2.2 μm	0.9 μm	2 ~ 3.5 μm	0.2 ~ 0.5 μm	~ 0.6 μm after development	~ 0.45 μm	1.5 μm
Index of Film at .633 μm	1.555	1.573	1.581	1.664	1.489 to 1.563, adjustable	1.59	1.618	~ 1.6	1.615
Attenuation at .633 μm	8 dB/cm	4 dB/cm	0.3 dB/cm	0.5 dB/cm	~ 0.2 dB/cm for 2 μm or thinner ~ 1.2 dB/cm for 3.5 μm film	~ 1 dB/cm			7 dB/cm
Reference	Ref. 26	Ref. 26	Ref. 26	Ref. 26	Ref. 27	Ref. 29	Ref. 25	Ref. 28	Ref. 26

Table 2. Optical Waveguides on Glass by r.f. sputtering

Substrate Material	Glass	Corning 8370	Glass	Soda-lime glass
Film Material	Corning 7059	Corning 8390	ZnO	Corning 7059
Sputtering Ambient	O_2	-	Ar and O_2	80% Ar, 20% O_2
Pressure	-	-	-	$1x10^{-3}$ to $3x10^{-3}$ Torr
R.F. Power Density	-	-	-	0.8 to 4.0 w/cm^2
Typical Film Thickness	.3 μm	.76 μm	1.59 μm	-
Index at .633 μm	1.62	1.73	1.973	1.53 to 1.58 (depending on r.f. power)
Attenuation at .633 μm	1 dB/cm	-	-	~ 1.8 dB/cm
Reference	Ref. 31	Ref. 32	Ref. 35	Ref. 33, 34

Table 3 Fabrication Parameters for Forming Ion-Exchanged Waveguides

Substrate	Soda-lime glass	Aluminosilicate	Soda-lime glass	Soda-lime glass	Soda-lime glass	Soda-lime glass	Soda-lime glass	Borosilicate glass
Ion Sources	$AgNO_3$ melts	KNO_3 melts	$AgNO_3$ melts	1% $AgNO_3$ in $NaNO_3$	Li_2SO_4, 80 mol.% K_2SO_4, 20 mol.%	Thermally evaporated Ag vapor	$AgNO_3$ or Ag Film	Mixture of $TlNO_3$, KNO_3 & $NaNO_3$
Exchanging ions	$Ag^+ \leftrightarrow Na^+$	$K^+ \leftrightarrow Na^+$	$Ag^+ \leftrightarrow Na^+$	$Ag^+ \leftrightarrow Na^+$	$Li^+ \leftrightarrow Na^+$	$Ag^+ \leftrightarrow Na^+$	$Ag^+ \leftrightarrow Na^+$	$Tl^+ \leftrightarrow K^+$ $Tl^+ \leftrightarrow Na^+$
Temperature (typical value)	225°-270°C (225°C)	360°-365°C	220°-350°C (280°C)	315°C	520°-620°C (575°C)	215°-245°C	170°-300°C (250°C)	530°C
Duration	24 hrs.	24 hrs.	16-256 min.	2 hrs.	1-17 min.	1-32 min.	15-120 min.	23 hrs. - 72 hrs.
Electric field	0	0	0	0	0	$(5\sim10)\times10^4$ v/m	$0\sim5\times10^5$ v/m	700 V/m
Δn at .633 μm	0.08	-	0.095	Depending on dilution	0.015	0.08	-	0.005 to 0.1
No. of Modes	8	1	multimodes	Depending on dilution	17	12	-	-
Attenuation at .633 μm	0.1 dB/cm	-	-	-	0.5-1.2 dB/cm	1 dB/cm	-	.1 dB/cm
References	Ref. 45	Ref. 45	Ref. 47	Ref. 51	Ref. 48	Ref. 52	Ref. 49	Ref. 44

Table 4 Fabrication parameters for in-diffuses

$LiNbO_3$ and $LiTaO_3$ waveguide

Substrate	$LiNbO_3$	$LiNbO_3$	$LiTaO_3$	$LiTaO_3$	$LiTaO_3$	$LiTaO_3$
Metal to be diffused (typical)	Ti,V,Ni (Ti)	Ti**	Nb	Nb	Cu	Cu or CuO
Thickness before diffusion	200-800Å	100-500Å	150-1500Å	200-1300Å	5000Å	
Temperature	850-1000°C (960°C for Ti)	1050°C	1100°C*	1200°C *	800°C	550°C
Duration	6 hrs.	5 hrs.	~ 6 hrs.	4-18 hrs.	1 hr.	1 hr.
Atmosphere	Flowing Ar, O_2	Flowing O_2	Ar	Ar	Air or Ar	Air
Electric field during diffusion	0	0	0	0	0	10^4 V/m
Diffusion depth	1-3 μm	1-2 μm	-	-	120 μm	25 μm
Δn at .633 μm	Δn_o~0.01 Δn_e~0.04	-	Δn_o~0.01	Δn_o~0.018 to 0.03	Δn_o~0.003	Δn_o~0.005 Δn_e~0.005
Attenuation at .633 μm	~1 dB/cm	-	-	1.2 dB/cm	-	-
References	Ref. 60	Ref. 64	Ref. 55	Ref. 57	Ref. 56	Ref. 56

*Poled following diffusion

**Purity of Ti: 99.97%

NAC TR-2318

DISTRIBUTION LIST

NAC Security Vault, D/915.4

All copies for storage and distribution as follows

Commander, Naval Air Development Center
Warminster, PA 18974
Attn: Technical Library (Code 8131)
R. Desipio
L. Smith
E. Ressler

Commander, Naval Air Systems Command
Washington, DC 20361
Attn: AIR-360A (F. Lueking)
AIR-360B (B. Zempolich)
AIR-360 (C. D. Caposell)
AIR-00D4 (2 cys)
AIR-5162C (5 cys)
AIR-310B (J. Willis)
AIR-533F (D. Meyers)
Technical Library

Commander, Naval Sea Systems Command
Washington, DC 20360
Attn: Technical Library

Commander, Naval Ocean Systems Center
271 Catalina Boulevard
San Diego, CA 92152
Attn: Technical Library (Code 4473B)

Commanding Officer, Naval Ordnance Station
Indian Head, MD 20640
Attn: Technical Library

Superintendent, Naval Postgraduate School
Monterey, CA 93940
Attn: Technical Library

Director, Naval Research Laboratory
Washington, DC 20375
Attn: Code 5216
Code 2627 (T. Giallorenzi)

Commander, Naval Weapons Center
China Lake, CA 93555
Attn: H. Blasic

Bell Telephone Laboratories, Inc.
Mountain Avenue
Murray Hill, NJ 07971
Attn: Technical Library

Bell Telephone Laboratories, Inc.
Whippany Road
Whippany, NJ 07981
Attn: Technical Reports Center (Rm. 2A-160)

Honeywell Aerospace Division
13350 U.S. 19
St. Petersburg, FL 33733
Attn: Technical Library

Honeywell Systems & Research Center
Research Department
2345 Walnut Street
Roseville, MN 55113
Attn: Technical Library

Hughes Aircraft Company
500 Superior Avenue
Newport Beach, CA 92660
Attn: Technical Library

RCA Corporation
RCA Laboratories
Princeton, NJ 08540
Attn: Technical Director

Sandia Laboratories
P. O. Box 5800
Albuquerque, NM 87115
Attn: Technical Library 3141

Headquarters, U. S. Marne Corps
Washington, DC 20380
Attn: Scientific Advisor (Code RD-I)

NASA, Marshall Space Flight Center
Huntsville, AL 35812
Attn: Technical Library

NASA, Manned Space Flight Center
Houston, TX 77058
Attn: Technical Library

National Bureau of Standards
Building 225, Room A-305
Washington, DC 20234
Attn: T. Leedy

Director, National Security Agency
Fort George G. Meade, MD 20755
Attn: Technical Library

University of California
Department of Engineering
Los Angeles, CA 90024
Attn: Electrical Engineering Department

School of Electrical Engineering
Purdue University
West Lafayette, IN 47907
Attn: Dr. Robert L. Gunshor

Office of The Undersecretary of Defense
for Research and Engineering
(Electronics and Physical Sciences)
Washington, DC 20361
Attn: J. Feinstein, Room 3D1079

Air Force Avionics Laboratory
Wright-Patterson Air Force Base
Dayton, OH 45433
Attn: AFAL/DME

Air Force Materials Laboratory
Wright-Patterson Air Force Base
Dayton, OH 45433
Attn: J. K. Erbacher (AFWAL/MLTE)

Westinghouse Electric Corporation
Advanced Technology Laboratory
P. O. Box 1521
Baltimore, MD 21203
Attn: D. Mergerian, M.S. 3714

Lawrence Radiation Laboratory
P. O. Box 808
Livermore, CA 94550
Attn: Technical Information Dept., L-3

Texas Instruments, Incorporated
Central Research Laboratories
P. O. Box 225936, M.S. 105
Dallas, TX 75265
Attn: Dr. Charles D. David, Jr.
Technical Library

DDC, Alexandria, VA	12

NAC:

765	2
800	1
810	1
811 (R. Katz)	1
813	1
813 (K. Jones)	1
960	1
963 (G. Magee)	1
915.4	25


DATE
ILME